Symmetry and Entropy of One-Dimensional Legal Cellular Automata

Yamasaki, Kazuhito
Nanjo, Kazuyoshi Z.
Chiba, Satoshi

(Citation)
Complex Systems,20(4):351-361

(Issue Date)
2012

(Resource Type)
journal article

(Version)
Version of Record

(URL)
https://hdl.handle.net/20.500.14094/90006377

Symmetry and Entropy of One-Dimensional Legal Cellular Automata

Kazuhito Yamasaki

Department of Earth and Planetary Sciences, Kobe University
Nada, Kobe, 657-8501, Japan

Kazuyoshi Z. Nanjo

Earthquake Research Institute, University of Tokyo, 1-1-1
Yayoi, Bunkyo-ku, 113-0032, Tokyo, Japan

Satoshi Chiba

Department of Ecology and Evolutionary Biology, Tohoku University
Aobayama, Sendai, 980-8578, Japan

The one-dimensional legal cellular automata (CAs) used in Wolfram's original classification from a viewpoint of symmetropy (an object related to symmetry and entropy) are quantified. For this quantification, the discrete Walsh analysis that expresses the two-dimensional discrete pattern in terms of the four types of symmetry is used. The following was found. (1) The relationship between symmetry and entropy of the CA patterns corresponds to the three qualitative classes of CAs: II, III, and IV. (2) The change in symmetropy shows that class IV (complex) exists between class II (periodic) and class III (chaotic). As an application of these findings, the scale dependence of the symmetropy of the CA patterns is considered, and it is shown that class IV is useful for drawing complicated patterns when the system must keep the number of cells low.

1. Introduction

Theoretical interest has been expressed in the symmetry and entropy of cellular automata (CAs) [1–4]. For example, the topological or metric entropy is useful for the well-known classification of the CAs into four classes: I (fixed point), II (periodic), III (chaotic), and IV (complex) [5]. However, the symmetry in abstract algebra is attractive in the study of the CA's rule [6–8]. This paper concentrates on the geometric symmetry in the discrete pattern caused by the CA's rule, and suggests a holistic approach to the four classes of the CA from the viewpoint of symmetropy (an object related to symmetry and entropy). For this, we use the discrete Walsh analysis (Figure 1(a); see also p. 573 in [1]), which has been used to express two-dimensional discrete patterns as the superposition of the four types of basic symmetry [9, 10] (Figure 1(b); the details are given in Section 3).

https://doi.org/10.25088/ComplexSystems.20.4.351

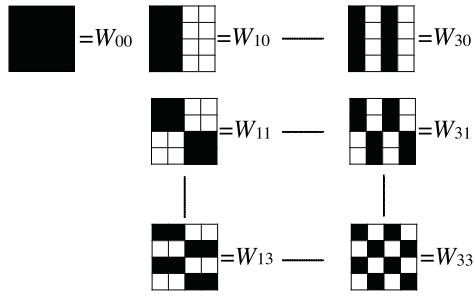

(a)

W_{mn}		m: even	m: odd
n	even	double symmetry $P4$	horizontal symmetry $P2$
n	odd	vertical symmetry $P1$	centrosymmetry $P3$

(b)

Figure 1. (a) Examples of the two-dimensional discrete Walsh function for $N \times N = 2^2 \times 2^2 = 4 \times 4$. Black represents $+1$ and white signifies -1. See also p. 573 in [1]. (b) Four types of symmetry in the sense of the discrete Walsh function. See Section 3 for details.

The Walsh approach is useful for analyzing the phase transition of discrete patterns, such as microfracturing and cell–cell adhesion [11–13]. Phase transitions are also observed in CA patterns [1, 14]. For example, the Langton parameter shows that the phase transition from periodic (class II) to chaotic (class III) through the complex (class IV) is recognized in the CA's rule space [15]. Although the so-called "edge of chaos" in [15] may be an artifact of the mathematical techniques [16], the phase transition in the CA is of scientific and practical interest in various subjects. Here we consider the phase transition of the CA from the viewpoint of symmetropy. For this, we derive the relation between symmetry and entropy in classes II, III, and IV. As an application, we discuss how the number of cells affects the symmetry and entropy of the CA patterns.

The structure of this paper is as follows. In Section 2, we explain data on the one-dimensional legal CAs. In Section 3, we briefly review the discrete Walsh analysis for estimating entropy and symmetry of the CA patterns. In Section 4, we describe the results. In Section 5, we

https://doi.org/10.25088/ComplexSystems.20.4.351

discuss the results and consider the relationship between the entropy and symmetry of the CA patterns from the viewpoint of phase transition and scale dependence. Section 6 is devoted to the conclusions.

2. Data

For simplicity, this paper concentrates on the classical CAs in the well-known Wolfram classification [5], that is, the one-dimensional legal CAs that obey the 32 possible legal totalistic rules. The totalistic rules involve nearest and next-nearest neighbors, and each cell has two possible colors: white (color 0) and black (color 1). Wolfram [5] discovered that while the patterns obtained with different rules all differ in detail, they appear to fall into four qualitative classes:

> Class I: Evolution leads to a homogeneous state (fixed point) (realized for codes 0, 4, 16, 32, 36, 48, 54, 60, and 62).
>
> Class II: Evolution leads to a set of separated simple stable or periodic structures (periodic) (codes 8, 24, 40, 56, and 58).
>
> Class III: Evolution leads to a chaotic pattern (chaotic) (codes 2, 6, 10, 12, 14, 18, 22, 26, 28, 30, 34, 38, 42, 44, 46, and 50).
>
> Class IV: Evolution leads to complex localized structures, sometimes long-lived (complex) (codes 20 and 52).

In this paper, we do not use all codes in class I because the patterns are trivial (i.e., most of the cells are white or black). Because the symmetry is related to the scale [12], we change the size (the number of cells) of the CA pattern. That is, the CAs are composed of 2^k sites where the positive integer k is shifted from $k = 3$ to $k = 7$, and iterated during 2^k time steps. (We do not use the cases $k = 1, 2$ because the number of cells is too small in this case.) After all, the total number of cells of the CA pattern is the product of the number of the sites and the number of the time steps: $2^k \times 2^k$, where $k = 3 \sim 7$. The initial state is taken as disordered, with each site having values 0 (white cell) and 1 (black cell) with independent equal probabilities. We run the CA program 100 times in a code with fixed k (i.e., we obtain 100×5 patterns for each code because k is shifted from 3 to 7). As described in Section 3, we estimate the entropy E and symmetry S of the patterns for each code and k and use the mean values of E and S as the characterization of the patterns.

3. Method: The Discrete Walsh Analysis

As details of the mathematical procedures of the discrete Walsh analysis were given in previous papers [9, 11], only a brief outline is described below. The Walsh function $\mathrm{wal}(r, x)$ of order r and argument x can be represented over the interval $0 \le x < 1$ as follows:

https://doi.org/10.25088/ComplexSystems.20.4.351

$\mathrm{wal}(r, x) = \prod_{i=0}^{m-1} \mathrm{sgn}\left[\left(\cos 2^i \pi x\right)^{r_i}\right]$, where $r_i = 0$ or 1, $r = \sum_{i=0}^{m-1} r_i 2^i$, and m is the smallest positive integer such that $2^m > r$. Dyadic addition of non-negative integers r and s is defined as $r \oplus s = \sum_{i=0}^{f} |r_i - s_i| 2^i$, where $r = \sum_{i=0}^{f} r_i 2^i$ and $s = \sum_{i=0}^{f} s_i 2^i$. Consequently, the product of the two Walsh functions is given by $\mathrm{wal}(r, x)\,\mathrm{wal}(s, x) = \mathrm{wal}(r \oplus s, x)$. From this multiplication, the Walsh functions can be shown to form an orthonormal set. In this case, we can define the Walsh transform just like the Fourier transform.

The two-dimensional discrete Walsh function can be represented in matrix form as $[W_{mn}(i, j)]$, where $W_{mn}(i, j)$ is the value of the $(m, n)^{\text{th}}$-order Walsh function in the i^{th} row cell in the j^{th} column. Patterns used in this paper are restricted to square matrices, each consisting of $N \times N = 2^k \times 2^k$ square cells, where k is a positive integer and takes the range $3 \sim 7$ (see Section 2). This pattern can be written as $\left[x_{ij}\right]$, where x_{ij} is the value of the gray level in the i^{th} row cell in the j^{th} column and $i, j = 0, 1, \ldots, N-1$. If just two gray levels exist, for example, "black" and "white," x_{ij} is usually represented by 1 and 0, respectively (Figure 1(a); see also p. 573 in [1]). The two-dimensional discrete Walsh transform of the pattern $\left[x_{ij}\right]$ is given by

$$a_{mn} = \frac{1}{N^2} \sum_{i=0}^{N-1} \sum_{j=0}^{N-1} x_{ij}\, W_{mn}(i, j)$$

where $m, n = 0, 1, 2, \ldots, N-1$. The functions a_{mn} and $(a_{mn})^2$ are the two-dimensional Walsh spectrum and power spectrum, respectively. The Walsh power spectrum can be normalized as follows:

$$p_{mn} = \frac{(a_{mn})^2}{K}, \tag{1}$$

with $K = \sum_{m=0}^{N-1} \sum_{n=0}^{N-1} (a_{mn})^2 - (a_{00})^2$. In this case, we obtain

$$\sum p_{mn} = 1, \tag{2}$$

where the sum is taken over all ordered pairs (m, n) for $0 \le m, n \le N-1$, except for $(m, n) = (0, 0)$.

The spatial pattern is considered as an information source consisting of dot patterns. The dot patterns emitted from the source are assumed to occur with the corresponding probabilities given by equation (1). Applying the entropy function in information theory to the normalized power spectrum p_{mn}, we obtain the information entropy concerned with the following pattern:

$$E = -\frac{1}{\log_2\left(N^2 - 1\right)} \sum_{m=0}^{N-1} \sum_{n=0}^{N-1} p_{mn} \log_2 p_{mn}, \tag{3}$$

https://doi.org/10.25088/ComplexSystems.20.4.351

where $\log_2(N^2 - 1)$ is the normalization constant. In this case, E ranges from 0 to 1 bit. If the value of a certain component is larger than the values of the other components, equation (3) shows that E decreases, that is, the pattern becomes systematic. If, however, the values of the components are almost equal to each other, E increases, that is, the pattern becomes random.

Next, we consider the information entropy resulting from the symmetry of the pattern. Because the two-dimensional Walsh functions can be easily divided into four types of symmetry (Figure 1(b)), equation (2) can be rewritten as

$$\sum_{i=1}^{4} P_i = 1, \tag{4}$$

where

$$\text{vertical symmetric component: } P_1 = \sum_{\substack{m=\text{even},\\ n=\text{odd}}} p_{m\,n}, \tag{5}$$

$$\text{horizontal symmetric component: } P_2 = \sum_{\substack{m=\text{odd},\\ n=\text{even}}} p_{m\,n}, \tag{6}$$

$$\text{centrosymmetric component: } P_3 = \sum_{\substack{m=\text{odd},\\ n=\text{odd}}} p_{m\,n}, \tag{7}$$

$$\text{double symmetric component: } P_4 = \sum_{\substack{m=\text{even},\\ n=\text{even}}} p_{m\,n}. \tag{8}$$

When the spatial pattern is regarded as an information source consisting of four types of symmetry, the corresponding probabilities are given by equations (5) to (8). Applying the entropy function in information theory to these four symmetric components, we obtain

$$S = -\sum_{i=1}^{4} P_i \log_2 P_i. \tag{9}$$

Equations (4) and (9) show that S ranges from 0 to 2 bits. Because this entropy relates to the symmetry, it is called symmetropy [9]. The

https://doi.org/10.25088/ComplexSystems.20.4.351

symmetropy can be considered a quantitative and objective measure of symmetry. If the value of a certain component is larger than the values of the other three components, the pattern is rich in symmetry related to the certain component. In this case, equation (9) shows that S decreases. Conversely, if the values of the four components are almost equal to each other, the pattern is poor in symmetry and S increases.

In the sense of the discrete Walsh analysis, the symmetry of a pattern is not necessarily correlated with entropy of the pattern, as shown in Figure 2 (see [13] for more details). However, previous studies have concentrated on the symmetry [11, 12]. In this case, we cannot quantify the difference between the patterns that have the same symmetry but different entropy. Therefore, the possibility exists that we overlooked important geometric information in the CA patterns. Hence in this paper, we estimate not only the symmetry but also the entropy of the CAs.

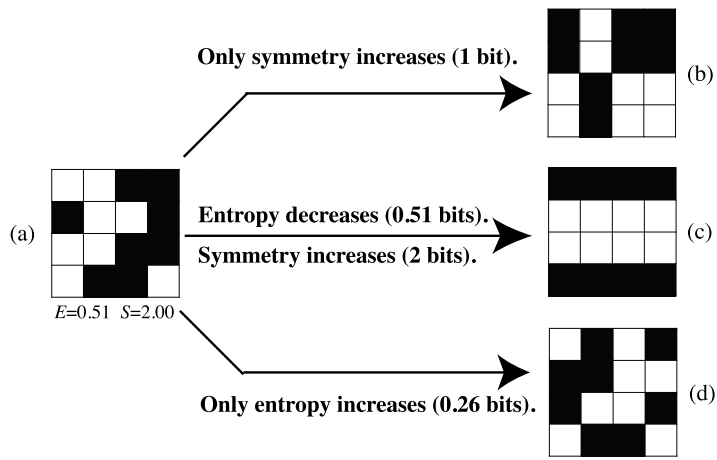

Figure 2. Symmetropy (S) and entropy (E) of samples. Figure 2(a) → 2(b): the pattern restores the particular symmetry (S decreases) to maintain the randomness (constant E). Figure 2(a) → 2(c): the pattern becomes systematic (E decreases) with the predominance of particular symmetry. Figure 2(a) → 2(d): the pattern becomes random (E increases) to maintain the degree of symmetry (constant S). Data from [13].

4. Results

Figure 3(a) shows the symmetropy S and the entropy E for the CA patterns of each code with $k = 7$. The square indicates class II, the triangle indicates class III, and the cross indicates class IV. All results have been rounded to no more than seven significant figures. As a whole, the relationship between S and E can be described as a linear

https://doi.org/10.25088/ComplexSystems.20.4.351

equation. However, each class exhibits a unique relationship between S and E. In class III (chaotic), S remains constant and E varies compared to the other classes. The code 52 in class IV (complex behavior) seems to show some deviation from the linear equation. These results almost hold for other k values.

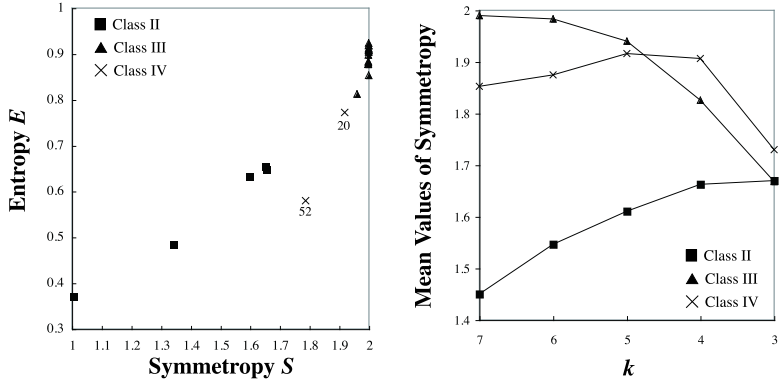

(a) (b)

Figure 3. (a) The relationship between the symmetropy and the entropy for class II (square), class III (triangle), and class IV (cross). The numbers 20 and 52 represent the code number. (b) The plot of the mean value of the symmetropy for each class against the scale parameter k.

Figure 3(a) also shows that the symmetropy of class IV is held between classes II and III. In the other k values (≥ 5), this relationship almost holds, as shown in Figure 3(b). Figure 3(b) shows plots of the mean values of symmetropy for each class against the k value. With a decrease in k (i.e., a decrease in the number of cells), the symmetropy of class II increases, that of class III decreases, and that of class IV remains almost constant. As a result, the symmetropy of class IV is held between classes II and III from $k = 7$ to $k = 5$. For the smallest case ($k = 3$), all of the classes almost took the same value.

Figure 4 shows plots of the mean values of the concrete symmetries: vertical symmetry (P_1), horizontal symmetry (P_2), centrosymmetry, and double symmetry (P_4) for each class against the scale k. When $k \geq 5$ (i.e., when enough cells were present), concrete symmetries of class IV were held between those of class II and those of class III, except for the vertical symmetry (P_1).

https://doi.org/10.25088/ComplexSystems.20.4.351

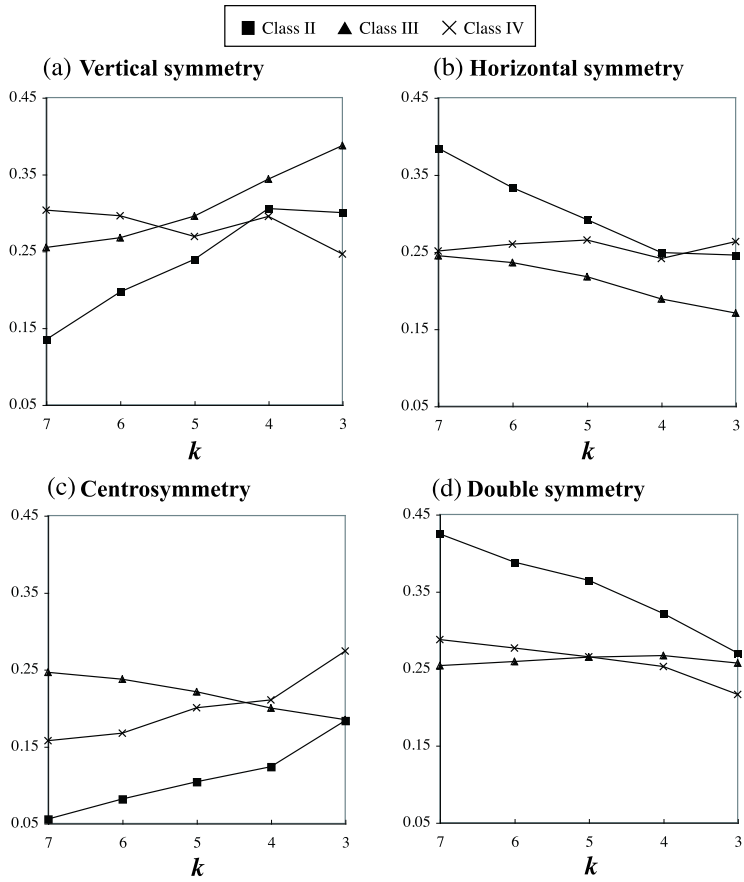

Figure 4. Plot of the four symmetry types against the scale parameter k. (a) Vertical symmetry (P_1). (b) Horizontal symmetry (P_2). (c) Centrosymmetry (P_3). (d) Double symmetry (P_4). The square indicates class II, the triangle indicates class III, and the cross indicates class IV.

5. Discussion

Wolfram [5] discovered that one-dimensional legal CAs appear to fall into four qualitative classes—class I (fixed point), class II (periodic), class III (chaotic), and class IV (complex)—and considered their behavior from a viewpoint of entropy. Here we considered the symmetrical property of CAs and showed that these classes have peculiar values of symmetropy S and entropy E (Figure 3(a)). This means that the algebraic rules for CAs restrict not only the entropy but also the symmetry of the CA patterns, in the sense of the discrete Walsh analysis.

https://doi.org/10.25088/ComplexSystems.20.4.351

Recently, some investigations have been conducted on the uniqueness of the code 52, such as the dynamic behavior exhibited by the "gliders" [17, 18] and the global equivalence classification [19]. Hence, discussing the uniqueness of code 52 in the context of the discrete Walsh analysis is intriguing. Figure 3(a) shows that the relationship between S and E can be described by a linear equation in general. In class IV, code 20 is on a straight line, but code 52 shows some deviation from this line due to the lower entropy. Class III also shows deviation from a straight line, but this may be attributable to the fact that the maximum value of S is 2.0 bits. Therefore, code 52 is essentially unique in the entropy. In this case, Figure 3(a) shows that code 52 is useful for drawing relatively regular patterns (lower entropy) with middle symmetric properties (middle symmetropy).

Next, we discuss the phase transition of the CA patterns. Langton showed the phase transition of class behavioral regimes with increasing Langton parameters [14–16]. The Langton parameter suggested on average a phase transition from class II to class III through class IV. (Of course, a specific value of the Langton parameter can be associated with more than one class, so the parameter reflects the average behavior of a class of rules [14].) Symmetropy has been applied to the analysis of the phase transition of various phenomena such as rock fragmentation [11, 12] and cell–cell adhesion [13], so discussing this point further here is relevant. Figure 3(a) shows that the symmetropy of class IV is in the transition area between that of classes II and III. To understand this, we extracted the concrete symmetry from the CA pattern for each class, as in Figure 4. We found in Figures 4(b), (c), and (d) that several symmetries of class IV are also held in classes II and III when $k \geq 5$ (i.e., when enough cells are present). This implies that the transition from class II to class III through class IV can be also recognized in the hidden symmetry of the CA patterns. In Figure 4(a), when $k \geq 6$, the prominence of the vertical symmetry in class IV appears to reflect the long-range correlation of class IV.

This analysis holds when the system has a large enough number of cells: $k \geq 5$ or $k \geq 6$. In nature, especially in biology, the number of cells is not infinite because the cost of forming cells is finite. How is the number of cells, characterized by the scale parameter k, related to symmetry in the discrete patterns? Figure 3(b) shows that when the number of cells decreases, the regular (class II) and random (class III) patterns approach each other. This scale dependence of the symmetropy has also been observed in physical systems, for example, fracturing in rock experiments [12]. With a decrease in scale, the symmetropy of the regular fracture pattern (nucleation of the fracturing process) increases, and that of the random fracture pattern (the pre- and post-nucleation phases) decreases. In summary, the scale dependence of the patterns caused by classes II and III is also observed in the fracturing process. However, Figure 3(b) shows that the pattern caused by class IV almost has the same symmetropy. This scale inde-

https://doi.org/10.25088/ComplexSystems.20.4.351

pendence has not been observed in the fracturing process [12]. This uniqueness of the class IV rule is useful for drawing complicated patterns when the system must keep the number of cells low. For example, in biological systems one must sometimes draw complicated patterns while reducing the cost of forming cells.

6. Conclusions

Our main conclusions are as follows. (1) The discrete Walsh analysis shows that the relationship between the symmetry and the entropy of the cellular automaton (CA) patterns correspond to the class of the CA. (2) The change in symmetropy shows that class IV is held between classes II and III. This implies the transition from the periodic (class II) to the chaotic (class III) through the complex (class IV) just as previous studies have indicated. (3) The scale dependence of the symmetropy of class IV shows that this class is useful for drawing complicated patterns when the system must keep the number of cells low.

References

[1] S. Wolfram, *A New Kind of Science*, Champaign, IL: Wolfram Media, Inc., 2002.

[2] H. Akin, "The Entropy of Linear Cellular Automata with Respect to Any Bernoulli Measure," *Complex Systems*, **18**(2), 2009 pp. 237–244.

[3] J. R. Sanchez and R. Lopez-Ruiz, "Symmetry Pattern Transition in Cellular Automata with Complex Behavior," *Chaos, Solitons & Fractals*, **37**(3), 2008 pp. 638–642. doi:10.1016/j.chaos.2006.09.052.

[4] H. V. McIntosh, *One Dimensional Cellular Automata*, Beckington, UK: Luniver Press, 2009.

[5] S. Wolfram, "Universality and Complexity in Cellular Automata," *Physica D: Nonlinear Phenomena*, **10**(1–2), 1984 pp. 1–35. doi:10.1016/0167-2789(84)90245-8.

[6] K. Cattell and J. C. Muzio, "Partial Symmetry in Cellular Automata Rule Vectors," *Journal of Electronic Testing: Theory and Applications*, **11**(2), 1997 pp. 187–190. doi:10.1023/A:1008226724350.

[7] H. Moraal, "Highly Symmetric Cellular Automata and Their Symmetry-Breaking Patterns," *Physica D: Nonlinear Phenomena*, **148**(3–4), 2001 pp. 255–271. doi:10.1016/S0167-2789(00)00195-0.

[8] A. Enciso, "Symmetry in Cellular Automata," *Electromagnetic Phenomena*, **6**(2), 2006 pp. 234–236. http://www.emph.com.ua/17/pdf/enciso.pdf.

[9] E. Yodogawa, "Symmetropy, an Entropy-Like Measure of Visual Symmetry," *Perception and Psychophysics*, **32**(3), 1982 pp. 230–240.

https://doi.org/10.25088/ComplexSystems.20.4.351

[10] K. Z. Nanjo, H. Nagahama, and E. Yodogawa, "Symmetropy of Fault Patterns: Quantitative Measurement of Anisotropy and Entropic Heterogeneity," *Mathematical Geology*, **37**(3), 2005 pp. 277–293. doi:10.1007/s11004-005-1559-z.

[11] Y. Nishiyama, K. Z. Nanjo, and K. Yamasaki, "Geometrical Minimum Units of Fracture Patterns in Two-Dimensional Space: Lattice and Discrete Walsh Functions," *Physica A: Statistical Mechanics and Its Applications*, **387**(25), 2008 pp. 6252–6262. doi:10.1016/j.physa.2008.07.014.

[12] K. Yamasaki and K. Z. Nanjo, "A New Mathematical Tool for Analyzing the Fracturing Process in Rock: Partial Symmetropy of Microfracturing," *Physics of the Earth and Planetary Interiors*, **173**(3–4), 2009 pp. 297–305. doi:10.1016/j.pepi.2009.01.010.

[13] K. Yamasaki, K. Z. Nanjo, and S. Chiba, "Symmetry and Entropy of Biological Patterns: Discrete Walsh Functions for 2D Image Analysis," *BioSystems*, **103**(1), 2011 pp. 105–112. doi:10.1016/j.biosystems.2010.10.010.

[14] J. L. Schiff, *Cellular Automata: Discrete View of the World*, Hoboken, NJ: John Wiley & Sons, 2008.

[15] C. G. Langton, "Computation at the Edge of Chaos: Phase Transitions and Emergent Computation," *Physica D: Nonlinear Phenomena*, **42**(1–3), 1990 pp. 12–37. doi:10.1016/0167-2789(90)90064-V.

[16] M. Mitchell, J. P. Crutchfield, and P. T. Hraber, "Dynamics, Computation, and the 'Edge of Chaos': A Re-examination," in *Complexity: Metaphors, Models, and Reality* (G. A. Cowan, D. Pines, and D. Melzner, eds.), Reading, MA: Addison-Wesley, 1994 pp. 491–513.

[17] J. G. Freire and J. A. C. Gallas, "Synchronization and Predictability under Rule 52, a Cellular Automaton Reputedly of Class 4," *Physics Letters A*, **366**(1–2), 2007 pp. 25–29. doi:10.1016/j.physleta.2007.01.071.

[18] J. G. Freire, O. J. Brison, and J. A. C. Gallas, "Spatial Updating, Spatial Transients, and Regularities of a Complex Automaton with Nonperiodic Architecture," *Chaos*, **17**(2), 2007 p. 026113. doi:10.1063/1.2732896.

[19] S. Shen and J. Guan, "The Study of One-Dimensional Cellular Automata with Nearest-Nearest Neighborhoods," in *International Workshop on Chaos-Fractal Theories and Applications (IWCFTA10)*, Kunming, China, Piscataway, NJ: IEEE, 2010 pp. 232–236. doi:10.1109/IWCFTA.2010.29.

https://doi.org/10.25088/ComplexSystems.20.4.351